Observed Impact of Snow Cover on the Heat Balance and the Rise of Continental Spring Temperatures

Pavel Ya. Groisman,* Thomas R. Karl, Richard W. Knight

Analysis of satellite-derived snow cover, radiative balance, and surface air temperature over Northern Hemisphere extratropical land shows that the retreat of the Northern Hemisphere's extent of spring snow cover over the past 20 years parallels a change in the influence of snow cover on the radiative balance and an observed increase of spring temperatures over the same area. These results help explain why the long-term (20th century) increase in surface air temperature over Northern Hemisphere land has been greater in spring than in any other season relative to the interannual variability.

Snow on the ground has important effects on the Earth's heat balance, influencing the planetary albedo (α) and outgoing long-wave radiation (OLR), which then feed back (*1*) to surface temperature. In this report, we estimate the impact of interannual and decadal snow cover variability on the hemispheric heat balance and temperature over the past 20 years. Our study focuses on the northern extratropical land (NEL) (Fig. 1), where snow covers the ground at least once every 20 years for a week or more. This area encompasses 55% (54.2×10^6 km^2) of the land in the Northern Hemisphere and 21% of the entire hemispheric area.

We used four databases: (i) Northern Hemisphere weekly snow cover derived from National Oceanic and Atmospheric Administration (NOAA) satellites (*2*); (ii) monthly mean surface air temperatures (*3*); (iii) the Earth Radiation Budget Experiment (ERBE) planetary albedo and OLR measurements (*4*); and (iv) a gridded climatology of total cloud cover (*5*). We interpolated or reinterpolated all monthly data (radiative fluxes, surface air temperature, and cloudiness) onto the same grid cells (4081 cells) used for snow cover measurements (Fig. 1).

The extent of annual snow cover (Table 1) declined by ~10% over the Northern Hemisphere, including both North America and Eurasia, over the past 20 years. Trends over the three continental-scale regions (North America, Europe and West Asia, and East Asia) are all negative. The decline is related to the increase in the annual temperature over these regions (*2*, *6*). Most of the decrease occurred in the second half of the hydrological year (April to September) and was especially prominent in spring (April to May).

The ERBE data from 1984 to 1988 were used to develop a relation between the fraction of monthly snow cover (S) and each of the various components of the Earth heat balance (clear-sky and total albedo and OLR). Because temperature is often a good surrogate for other factors (besides snow cover), we grouped grid cells by monthly surface air temperature (in the range of ±0.5°C). For each set of cells, we retrieved the corresponding radiation components for clear-sky and all-sky conditions and subjected them to a regression analysis. We estimated $\partial\alpha/\partial S$ ($\partial OLR/\partial S$) as a function of temperature by regressing the mean monthly values of planetary albedo (OLR) and snow cover for grid cells grouped together by surface air temperature (*7*). These relations were used to estimate the impact of snow cover on the climate system over the past 20 years.

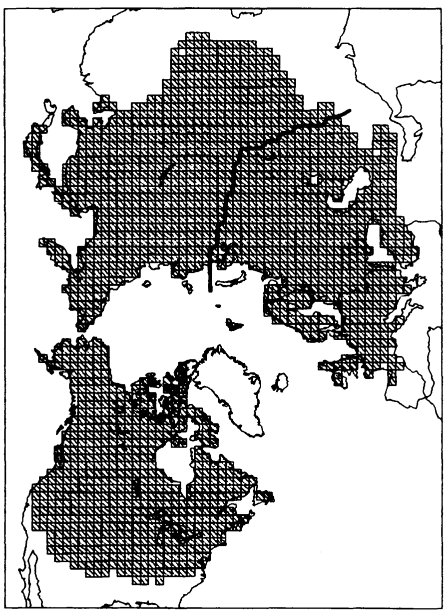

Fig. 1. Land area over Northern Hemisphere (except Greenland) where at least once during the past 20 years observations of weekly snow cover in January have reported the presence of snow cover (NEL). The spatial resolution of the observations is presented by the size of the grid cells. The bold line represents the partition of the Eurasian continent used in Table 1.

The radiative balance of an atmospheric column for each grid cell of the NEL is $RB = ASR - OLR$, where ASR (absorbed solar radiation) and OLR are determined at the top of the atmosphere (TOA), both being functions of TOA solar radiation (Q), temperature, cloudiness, and snow cover. The radiative balance equation can be expanded, and the main linear component affected by snow-cover variations is

$$RB_S = S\frac{\partial ASR}{\partial S} - S\frac{\partial OLR}{\partial S} + o(S) \quad (1)$$

where o(S) is the remainder of the Taylor series expansion, which is of minor importance in snow cover feedback and has been neglected. The values of ASR and OLR can be calculated by

$$ASR_{total} = Q[1 - \alpha_{clear}(1 - C) - C\alpha_{overcast}] \quad (2a)$$

and

$$OLR_{total} = OLR_{clear}(1 - C) + OLR_{overcast}C \quad (2b)$$

where C is the fraction of mean cloud cover over the grid cell (*8*). Substituting Eqs. 2 into Eq. 1 yields

$$RB_S = -S\,Q\partial[(1 - C)\,\alpha_{clear} + C\,\alpha_{overcast}]/\partial S - S\,\partial[OLR_{clear}(1 - C) + C\,OLR_{overcast}]/\partial S \quad (3)$$

where temperature, cloud cover, and snow cover can be considered to be independent variables. Equation 3 provides an estimate of the climatic feedback effect snow cover

Table 1. Linear trends, β, of snow cover over the NEL (1973–92), their standard errors, σ_β, and percent of interannual snow cover variability described by the trend (R^2). The value of β is reported at the 0.05 two-tail statistical significance level. Therefore, no data are reported for autumn (October to November) and winter (December to March).

Season	β (10^5 km^2/10 years)	σ_β (10^5 km^2/10 years)	R^2
	North America		
Spring	−7.4	2.8	28
Summer	−5.1	1.6	36
Annual	−4.3	1.4	34
	Europe and West Asia		
Spring	—	—	—
Summer	−2.1	0.5	53
Annual	−3.0	1.2	25
	East Asia		
Spring	−9.5	2.1	53
Summer	−4.6	1.3	40
Annual	−4.3	1.2	42
	All area		
Spring	−19.8	5.2	45
Summer	−11.8	3.1	45
Annual	−11.7	3.2	43

National Climatic Data Center, Federal Building, 37 Battery Park Avenue, Asheville, NC 28801.

*Permanent affiliation: State Hydrological Institute, 23 Second Line, St. Petersburg, 199053, Russia.

has on the regional heat balance. Clouds, their associated albedos, and OLR vary during the year, but the variation does not depend substantially on the presence or absence of snow cover; therefore, $\partial C/\partial S \approx 0$, $\partial OLR_{overcast}/\partial S \approx 0$, and $\partial \alpha_{overcast}/\partial S \approx 0$. These assumptions are approximately correct, except we shall show the last assumption not to be completely valid for temperatures below freezing. Equation 3 can then be simplified as

$$RB_S = -S\left(Q\frac{\partial \alpha_{clear}}{\partial S} + \frac{\partial OLR_{clear}}{\partial S}\right)(1 - C) \quad (4)$$

Integration of Eq. 4 over the NEL gives the hemispheric snow cover feedback of the RB (9).

The data (Fig. 2) show that snow cover increases the planetary albedo and, at the same time, suppresses OLR, which varies with surface temperature. These effects are especially apparent at low surface air temperatures because snow cover is likely to have different radiative characteristics at low temperatures and be more continuous. The relation depicted in Fig. 2A explains 25 to 30% of the spatial variance of clear-sky albedo (α_{clear}) for grid cells with mean temperature below 0°C, 15 to 20% of the variance for the grid cells with mean temperature from 0° to 5°C, and less than 10% of the variance for warmer temperatures. An estimate of the spatial variance of $\partial OLR_{clear}/\partial S$ as a function of the surface air temperature (Fig. 2B) explains 30 to 40% of the variance of OLR_{clear} for the grid cells with mean temperature below −5°C, 20 to 30% of this variance for the grid cells with mean temperature from −5° to 0°C, 8 to 15% of the variance for the grid cells with mean temperature from 0° to 4°C, and less than 4% of this variance for higher temperatures. The emissivity of snow-covered woodland or grassland is about 10% less than that of snow-free woodlands and grasslands (10). The sign of our estimates of $\partial OLR_{clear}/\partial S$ is consistent with this information.

We also applied the method used for the estimation of the derivatives $\partial \alpha_{clear}/\partial S$ and $\partial OLR_{clear}/\partial S$ to the OLR and albedo without regard to cloud cover (all-sky or "total" conditions). In this instance, however, the effects of clouds are included in the relation between the radiative balance and snow cover, so the concept of a partial derivative is no longer valid. If the influence of snow cover on the radiative fluxes is only manifested under clear-sky conditions, then the estimates of the $\partial \alpha_{total}/\partial S$ and $\partial OLR_{total}/\partial S$ (Fig. 2) should be equal to the values for clear-sky conditions when multiplied by a factor equal to $(1 - C)$. Our analysis shows that the sensitivity of the planetary albedo to snow on the ground for all-sky conditions is 5 to 50% higher than expected for temperatures below freezing (Fig. 2A). Furthermore, from −13° to −4°C, the relation describes a 5 to 10% larger portion of total variance between albedo and snow cover than the clear-sky relation. This apparent discrepancy may be a result of thin clouds, often registered by surface observers [and therefore, present in the data of Warren *et al.* (11)] in cold climates. Thin clouds are relatively transparent to the sunlight, allowing the snow cover to affect planetary albedo for cloudy-sky conditions. Regression estimates of $\partial OLR_{total}/\partial S$ for all-sky conditions are about one-sixth of those for clear-sky conditions and describe 5% or less of the total OLR variance. This decrease of sensitivity to snow cover is likely related to a combination of cloud and water vapor effects that interfere with the impact of snow cover on long-wave radiation. The effect of snow cover on OLR estimated from clear-sky long-wave fluxes characterizes an atmosphere significantly drier than that under all-sky conditions (12). We expect a stronger absorption of long-wave radiation by atmospheric water vapor under all-sky conditions, compared with that under clear skies, and a reduced impact of snow cover on the OLR. This partially explains the difference in the $OLR_{clear}(1 - C)$ versus OLR_{total} sensitivities. We cannot separate the effects of clouds and water vapor in the framework of our approach (13).

Year-by-year seasonal estimates of the snow-cover feedback on the radiative balance can be made with the results in Fig. 2, Eq. 4, and the observed snow cover. The time series of the interannual variations of RB_S from Eq. 4 (Fig. 3A and Table 2) (14) indicates that (i) despite the larger extent of snow cover in winter (December to March) compared to spring (April to May), the snow cover feedback of ASR in spring is just as large; (ii) the maximum impact of snow cover on OLR occurs in winter and has a

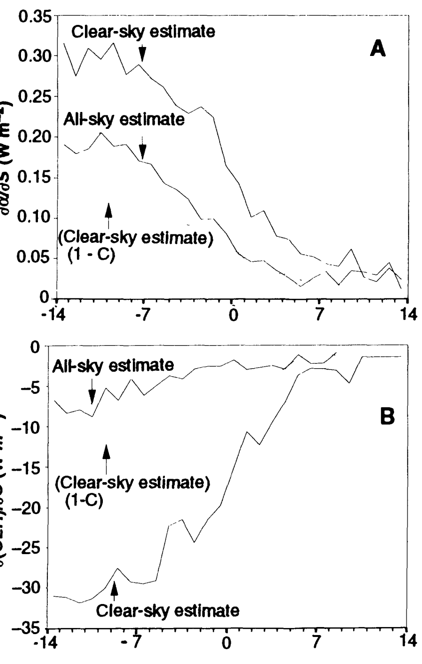

Fig. 2. (**A**) Sensitivity of clear-sky and total albedo to the snow cover extent ($\partial \alpha_{clear}/\partial S$ and $\partial \alpha_{total}/\partial S$) as functions of the mean surface air temperature. (**B**) Sensitivity of clear-sky and total OLR to the snow cover extent ($\partial OLR_{clear}/\partial S$ and $\partial OLR_{total}/\partial S$) as functions of the mean surface air temperature. Dashed lines are the clear-sky curves multiplied by $(1 - C)$, where $1 - C$ is the fraction of clear skies.

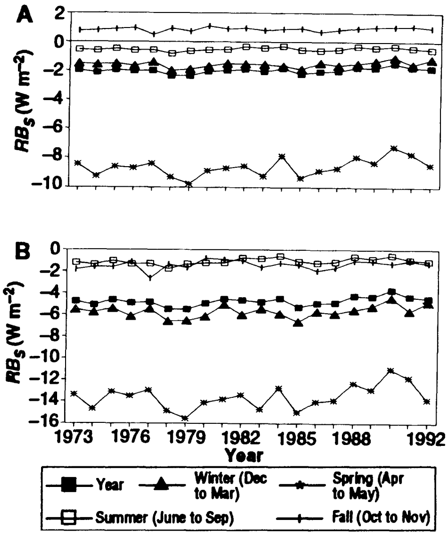

Fig. 3. Seasonal and annual impact of snow cover on the radiative balance over the NEL (RB_S) on the basis of (**A**) the clear-sky approach (Eq. 4) and (**B**) the all-sky ASR (from Eq. 5) and the clear-sky OLR (from Eq. 4) approaches.

Table 2. The impact of snow cover on the radiative balance over the NEL over the past 20 years. Mean values and interannual standard deviations are listed (on the basis of the clear-sky approach).

Season	Short-wave (ASR) ($W\ m^{-2}$)	Long-wave (OLR) ($W\ m^{-2}$)	Total (RB_S) ($W\ m^{-2}$)
Autumn	−3.1 ± 0.5	4.0 ± 0.3	0.9 ± 0.1
Winter	−11.2 ± 0.5	9.7 ± 0.3	−1.6 ± 0.2
Spring	−11.6 ± 0.8	3.0 ± 0.2	−8.6 ± 0.6
Summer	−0.7 ± 0.2	0.1 ± 0.04	−0.5 ± 0.1
Year	−6.4 ± 0.34	4.4 ± 0.16	−2.0 ± 0.20

Table 3. The impact of snow cover on the radiative balance over the NEL over the past 20 years. Mean values and interannual standard deviations are listed (on the basis of the all-sky approach). The last two columns pertain to the all-sky approach for the short-wave feedback (from Eq. 5) and to the clear-sky approach for the long-wave feedback (from Eq. 4).

Season	Short-wave (*ASR*) (W m^{-2})	Long-wave (*OLR*) (W m^{-2})	Total (RB_S) (W m^{-2})	
			All-sky *OLR*	Clear-sky *OLR*
Autumn	−5.4 ± 0.8	2.8 ± 0.2	−2.6 ± 0.6	−1.4 ± 0.4
Winter	−15.4 ± 0.8	5.3 ± 0.2	−10.0 ± 0.6	−5.7 ± 0.6
Spring	−16.6 ± 1.3	1.9 ± 0.1	−14.7 ± 1.2	−13.7 ± 1.1
Summer	−1.2 ± 0.3	0.2 ± 0.05	−1.1 ± 0.3	−1.1 ± 0.3
Year	−9.2 ± 0.56	2.6 ± 0.11	−6.6 ± 0.46	−4.8 ± 0.42

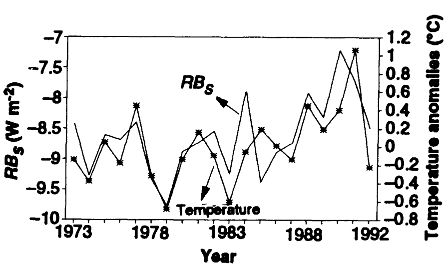

Fig. 4. Spring (April to May) impact of snow cover on the radiative balance (RB_S) and surface air temperature anomalies over the NEL; the correlation coefficient between these two time series is 0.72.

sign opposite that of the albedo; (iii) the effect of snow cover on the radiative balance is near zero during summer and autumn; and (iv) as a result of the above, the effect of snow cover on radiative balance is largest during spring (April to May). If instead of using Eq. 4, we use

$$RB_S = -S\left(Q\frac{\partial\alpha_{\text{total}}}{\partial S} + \frac{\partial OLR_{\text{total}}}{\partial S}\right) \quad (5)$$

where the estimates of $\partial\alpha_{\text{total}}/\partial S$ and $\partial OLR_{\text{total}}/\partial S$ relate to all-sky conditions, these conclusions remain unchanged, but the magnitude of the feedback on *RB* is different (Table 3 and Fig. 3B) (*15*).

In spring, the influence of snow cover on the radiative balance is especially prominent. The global retreat of the spring snow cover over the past 20 years (Table 1) has enhanced the warming in NEL. A change in the magnitude of *RB* of 1.0 W m^{-2} corresponds to an increase of surface air temperature of about 0.6°C on the basis of the sensitivity of the Earth climate system to radiative forcing estimated from climate models and satellite observations (*16*). The change in the annual *RB* as a result of snow cover over the NEL between 1979 and 1990 (two extremes) was 0.9 W m^{-2} (in spring 2.6 W m^{-2}). This corresponds to an increase of about 0.5°C in the annual surface air temperature over NEL (in spring, 1.5°C). Over the NEL, the actual difference in mean surface air temperature between these two years is 0.98°C and, in spring, 1.09°C. Thus, about 50% of the annual temperature difference of these two years (and much more in spring) may be related to snow cover feedback. Of course, advection distributes the excess radiation gain to other regions. The negative trend found in the summer snow cover (Table 1) is probably a residual stemming from the retreat of spring snow cover.

Jones and Briffa (*17*) found that over the past 100 years, there was a significant increase in global surface air temperature; century-long trends in surface air temperature were especially prominent over the land areas of the Northern Hemisphere during April and May. Our analysis indicates that there is a strong positive feedback between spring snow cover and the radiative balance over the NEL. During the 20th century, the global warming that has occurred in the spring is likely to have been significantly enhanced by corresponding changes in snow cover extent (Fig. 4). Thus, the transient effects of external climate forcing, such as greenhouse warming, may be especially prominent during spring in mid- and high-latitude lands of the Northern Hemisphere, where snow cover variations substantially affect the radiative balance.

REFERENCES AND NOTES

1. Climate-related variables can be loosely classified into three categories: forcings, feedbacks, and responses. The climate is forced by those conditions that directly affect other climate elements, the response variables. Changes in a response variable can sometimes affect other climate-related elements, providing feedback effects. In this sense, changes in snow cover force changes in the hemispheric radiative balance. Snow cover is often regarded as a feedback variable because changes in temperature affect snow cover, which then has a feedback effect on temperature.
2. The snow cover data consist of digitized maps of weekly snow cover prepared from visible imagery from NOAA polar-orbiting satellites supplemented with Geostationary Operational Environmental Satellite (GOES) and Meteosat satellite imagery [T. R. Karl *et al.*, *J. Clim.* **6**, 1327 (1993); M. Matson and D. R. Wiesnet, *Nature* **287**, 451 (1981); K. F. Dewey and R. R. Heim Jr., *Bull. Am. Meteorol. Soc.* **63**, 1132 (1982); D. A. Robinson *et al.*, *ibid.* **74**, 1689 (1993)]. The data incorporate many of the corrections recommended by D. A. Robinson *et al.* [*Proceedings of the 15th Annual Climate Diagnostics Workshop*, Asheville, NC, 29 October to 2 November 1990 (American Meteorological Society, Boston, MA, 1991), p. 219] and spans from October 1972 through September 1992. The spatial resolution varies with latitude, ranging from 20,643 km^2 at high latitudes to 42,394 km^2 at low latitudes. Each grid cell contains one bit of information for every week, indicating the absence or presence of snow cover. For each grid cell, the weekly snow cover was integrated over monthly and seasonal time scales.
3. Monthly temperatures (1972 to 1992) were selected from two archives: the Global Historical Climatology Network [R. S. Vose *et al.*, *Environ. Sci. Div. Publ. No. 3912* (Carbon Dioxide Information Analysis Center, Oak Ridge National Laboratory, Oak Ridge, TN, 1992)] and surface data from 376 Chinese stations, compiled by W. Wan-Lin and transferred to the U.S. National Climatic Data Center in the framework of a Bilateral Data Exchange between the Peoples Republic of China and the United States. A total of 1543 stations were used.
4. The ERBE monthly values of clear-sky and total radiative fluxes were used from the scanners with narrow field of view (albedo and outgoing infrared radiation). These data are gridded at a resolution of 2.5° and are available for November 1984 through December 1988 [B. R. Barkstrom, *Bull. Am. Meteorol. Soc.* **65**, 1170 (1984); B. R. Barkstrom *et al.*, *ibid.* **70**, 1254 (1989)].
5. Digital maps of the global distribution of total cloud cover (*11*) span from 1971 to 1981. We found that the spatial and temporal variations of the cloud cover are not correlated with variations of snow cover over the NEL. When snow is on the ground, clouds tend to have a small mean effect on the radiation fields at the TOA because both are cold and bright [H. L. Kyle *et al.*, *Bull. Am. Meteorol. Soc.* **74**, 815 (1993)]. For these reasons, we averaged the cloud cover over the 11-year period and used the averages in subsequent analyses.
6. D. A. Robinson and K. F. Dewey, *Geophys. Res. Lett.* **17**, 1557 (1990).
7. Other variables were added to the list of independent variables in a multiple linear-regression equation. This included the solar zenith angle and the temperature (which varies in the range of ±0.5°C). The estimates of $\partial\alpha/\partial S$ and $\partial OLR/\partial S$ are not significantly changed when any of these factors are incorporated into the equation.
8. The mean value of *C* is close to 0.6 and does not change with temperature.
9. We ignored the variations of the snow cover over sea ice and over Greenland.
10. A. Henderson-Sellers and P. J. Robinson, *Contemporary Climatology* (Longman Scientific, Harlow, United Kingdom, 1986).
11. S. G. Warren *et al.*, *NCAR Tech. Note 273 STR* (National Center for Atmospheric Research, Boulder, CO, 1986).
12. R. D. Cess *et al.*, *J. Geophys. Res.* **97**, 20421 (1992).
13. We grouped the data according to surface air temperature to estimate $\partial OLR/\partial S$ and found that under all-sky conditions, this temperature is a poor surrogate for other factors (besides snow cover) affecting *OLR*.
14. The numbers should be reduced by a factor of 0.21 or 0.55 if integrated over the Northern Hemisphere or the Northern Hemisphere land areas, respectively.
15. We believe that Eq. 4 (and therefore Fig. 3A and Table 2) provides better estimates and definition of the snow cover feedback of the radiative balance, whereas Eq. 5 provides less accurate results, especially for $\partial OLR/\partial S$ in all-sky conditions.
16. V. Ramanathan, B. R. Barkstrom, E. F Harrison, *Phys. Today* **42**, 22 (May 1989).
17. P. D. Jones and K. R. Briffa, *Holocene* **2**, 165 (1992).

18. Supported by the NOAA Office of Global Programs and a Department of Energy Office of Environmental Effects/NOAA National Climatic Data Center Interagency Agreement.

13 August 1993; accepted 18 November 1993